coatings

MDPI

Article

Finite Element Analysis (FEA) of the Stresses and Strains Occurring in Zirconia Crowns and Tooth Abutments Prepared With or Without a Shoulder Finish Line

Lucia Alexandra Drăghici [1,2], Raluca Monica Comăneanu [1,2,*], Ștefan Eugen Chirsanov-Capanu [1,2], Andrei Constantinovici [2], Anna Maria Pangică [2,*], Manuela Victoria Chivu [2], Mariana Roxana Ciobanu [1,2], Mihail Târcolea [3] and Laurența Lelia Mihai [2]

[1] Doctoral School of Dental Medicine, Titu Maiorescu University, 189 Calea Văcărești, 040051 Bucharest, Romania
[2] Department of Specialized Dental Medicine Disciplines, Faculty of Dental Medicine, Titu Maiorescu University, 67A Gheorghe Petrașcu Street, 031593 Bucharest, Romania
[3] Doctoral School of Materials Science and Engineering, National University of Science and Technology Politehnica Bucharest, 060042 Bucharest, Romania
* Correspondence: monica.comaneanu@prof.utm.ro (R.M.C.); anna-maria.pangica@prof.utm.ro (A.M.P.)

Abstract

This study aimed to evaluate the stress and strain at the interface between zirconia crowns and prepared tooth abutments, with or without a shoulder finish line. The main objective was to determine which of the two types of preparations provides a more favorable long-term prognosis, particularly in the case of single-unit crowns. The Finite Element Analysis (FEA) method was employed to assess the mechanical response of both zirconia and dentin under occlusal forces of 200 N, simulating physiological occlusion. Values from the literature for Young's modulus, Poisson's ratio, and Bulk modulus were introduced into the simulations for zirconia and tooth abutments. The simulations demonstrated that zirconia crowns, regardless of the preparation type, experienced higher stress than the tooth abutments. However, preparations with a shoulder finish line demonstrated superior biomechanical behavior. This study provides a detailed biomechanical analysis of zirconia crowns cemented onto tooth abutments prepared with or without a shoulder finish line, highlighting the importance of FEA in optimizing prosthetic design and material selection.

Keywords: finite element analysis (FEA); zirconia (zirconium dioxide); shoulder finish line preparation; preparation without a shoulder finish line

Check for updates

Academic Editor: Eugenio Velasco-Ortega

Received: 6 March 2026
Revised: 29 March 2026
Accepted: 8 April 2026
Published: 16 April 2026

Copyright: © 2026 by the authors. Licensee MDPI, Basel, Switzerland. This article is an open access article distributed under the terms and conditions of the Creative Commons Attribution (CC BY) license.

1. Introduction

Finite element analysis (FEA) is a method of numerical analysis that employs multiple calculation procedures [1]. FEA involves constructing a physical model corresponding to the problem to be solved, which will be decomposed into smaller constituent elements interconnected through "nodes". Material properties are assigned to the model, and external forces [2] and/or thermal variations are applied to it. The method is a valuable tool for evaluating the stress and strain that occur in the model. This is achieved without involving ethical considerations regarding experiments conducted on human models. Moreover, it is performed in a shorter time and at lower costs than those required for clinical studies [3,4].

FEA is an extremely advanced numerical technique, widely used in various engineering fields to analyze the mechanical behavior of complex structures. In dentistry, applying

FEA has become indispensable, having a significant impact on the research and development of materials used in prosthetic restorations [5]. FEA is capable of successfully estimating complex simulations involving geometric deformation and stress distribution, which are difficult or impossible to measure in vivo [6–13].

Biomechanical considerations are essential for the design of prosthetic restorations, and FEA can be integrated into the processing stages of CAD/CAM restorations to optimize their biomechanical performance [14]. In response to vertical and oblique biomechanical loads Zupancic et al. [15] studied the biomechanical performance of three-unit CAD/CAM fixed prostheses on short implants in the posterior mandible. The results demonstrated that the biomechanical response may vary depending on patient-specific parameters.

Zirconia exhibits highly variable values of resistance to stress loads [16], but FEA has confirmed that zirconia demonstrates a uniform stress distribution even under significant occlusal loads [17].

2. Materials and Methods

Two premolars extracted for orthodontic reasons were used in this study, which were prepared post-extraction: one with a shoulder finish line (A) and one without a shoulder finish line (B). The premolars were prepared for prosthetic restoration under simulated clinical conditions, following a clearly defined and standardized protocol. Initially, cylindrical diamond burs with a green ring were used to outline the guiding grooves and remove excess dental tissue, followed by the use of red-ring cylindrical diamond burs to refine the preparation. This stage involved both the removal of dental substrate and the shaping of the prosthetic abutments according to two distinct preparation designs—one with a shoulder finish line and one without. The finishing procedures used cylindrical diamond burs with a yellow ring. After that, the teeth were ready for the impression-taking phase preceding the fabrication of the prosthetic crowns.

The teeth were scanned using an intraoral scanner for digital impression, after which two zirconia crowns were cemented. Additionally, the specimens were subjected to computed tomography (CT) scanning to obtain accurate anatomical geometry. The obtained data were recorded in an STL file ("Standard Triangle Language" or "Standard Tessellation Language"). These were subsequently processed using Mimics Innovation Suite, Materialise NV.

The STL files were processed using the operations Remesh, Create Volume, Mesh in 3-matic (Leuven, Belgium), and later Export to ANSYS, (© ANSYS Inc., Houston, TX, USA) the dedicated software for finite element analyses (Figures 1 and 2).

The processing of information in Mimics Innovation Suite was carried out in discretization of CBCT (teeth) and STL (crowns). The main parameters in terms of nodes are presented in Table 1.

Table 1. Discretization details of the virtual premolar models used for FEA.

Element Types		**Quadratic Tetrahedron Semi Parabolic**	
		Elements	**Nodes**
With shoulder	Tooth	1678	3142
	Crown	1697	3323
Without shoulder	Tooth	1161	2249
	Crown	7780	14,501

The contact points must be placed in accordance with occlusal principles and with a normal occlusal scheme to offer a realistic and precise simulation. These principles ensure

the correct distribution of occlusal forces. The placement of the contact points was performed respecting the fundamental rules of functional occlusion. The contact points were positioned on the occlusal surface in the central fossa and on the tip of the buccal cusp in maximum intercuspation, while the inferior surface of the tooth was considered as fix support. A standard occlusal force of 200 N was applied in the simulation.

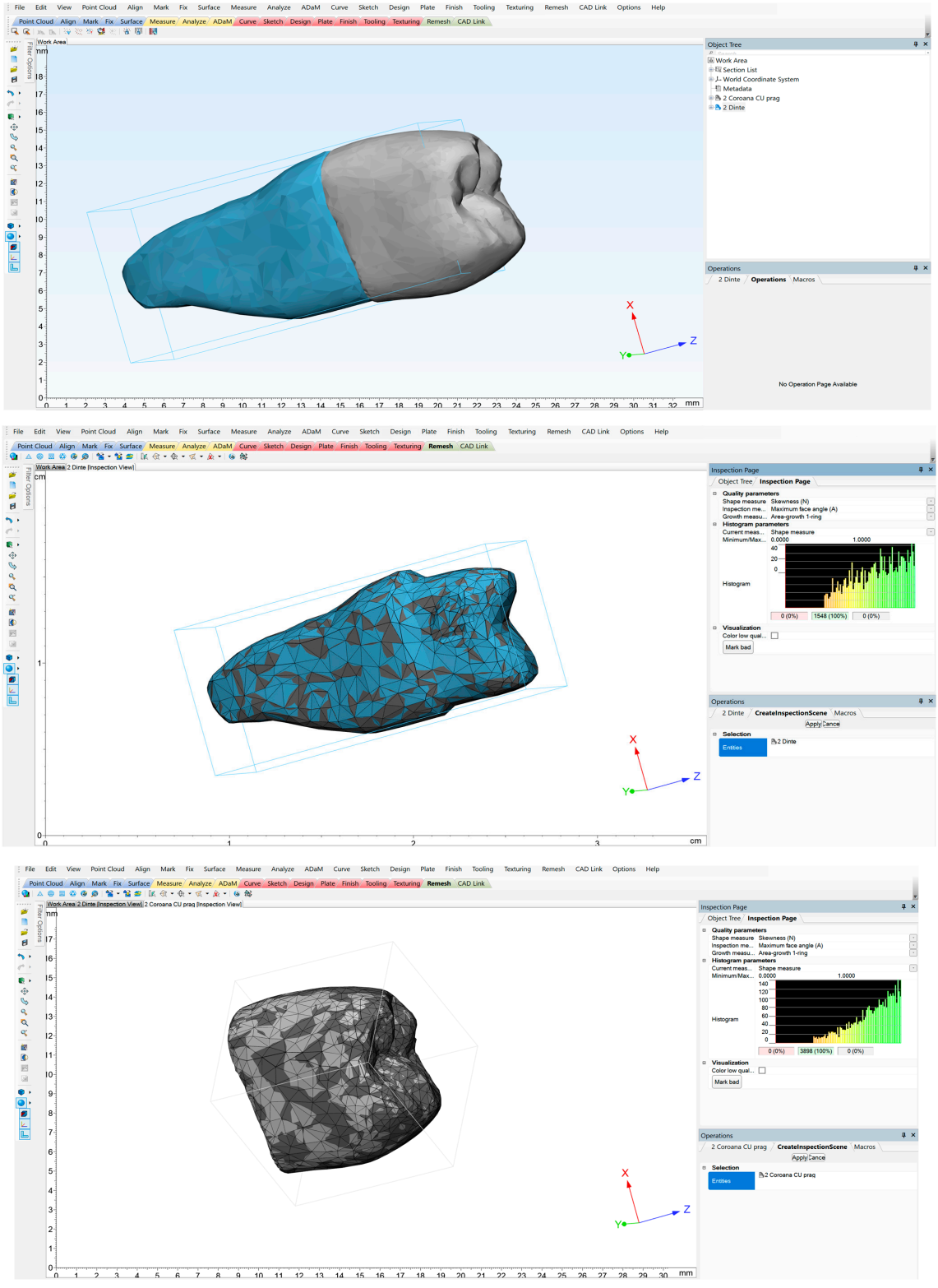


Figure 1. Processing stages with 3-matic © of the premolar prepared with a shoulder finish line.

https://doi.org/10.3390/coatings16040482

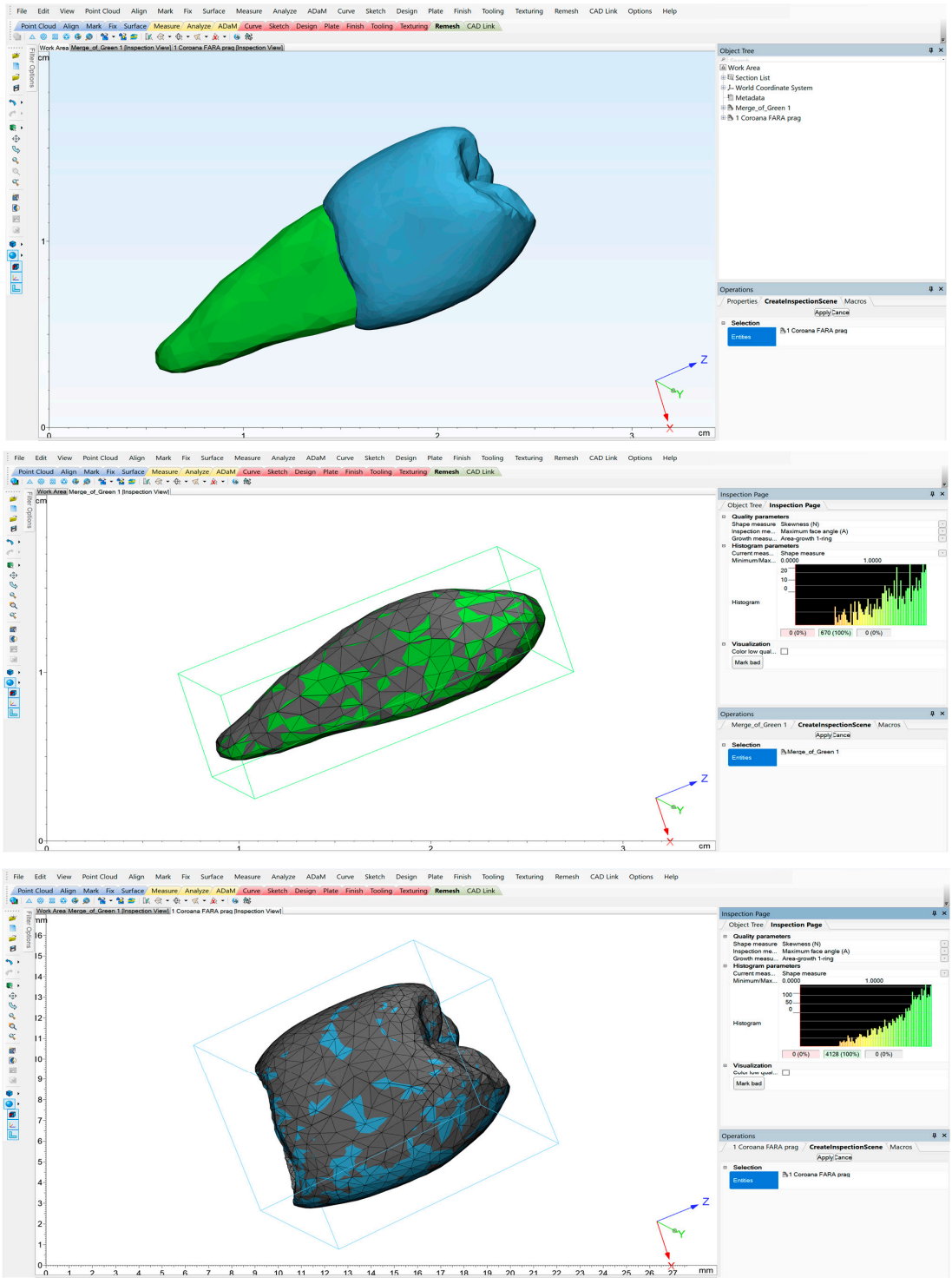


Figure 2. Processing stages with 3-matic © of the premolar prepared without a shoulder finish line.

The stress and strain were monitored for the tooth abutments and for the zirconia. The simulations required the introduction of the material constants, including Poisson's ratio and Young's modulus, selected based on validated values from the scientific literature (Table 2).

Table 2. Properties of the materials subjected to finite element analysis (FEA).

Material	Young's Modulus (MPa)	Poisson's Ratio (−)
Dentin	18,000	0.30
Zirconia	190,000	0.33

https://doi.org/10.3390/coatings16040482

The prosthetic crowns were analyzed under the action of concentrated forces applied in the previously defined contact areas, according to physiological occlusal forces, based on the STL files introduced and processed in 3-matic © Materialise NV(Mimics Innovation Suite ©, Materialise, Leuven, Belgium), Materialise NV, and subsequently exported intoANSYS 17 ©, Ansys, Inc., American multinational company, the dedicated software for finite element analysis.

The FEA was carried out at a constant environmental temperature of 36 °C, applying an experimental force of 200 N in the *Z* axis on both models, with and without a shoulder finish line, according to the principles of functional occlusion.

3. Results

When applying the 200 N force to the analyzed dental crowns, the following parameters were calculated for each, on the *Z* axis: total deformation; deformation on the X, Y, and Z directions; equivalent elastic strain; maximum principal elastic strain; minimum principal elastic strain; elastic strain intensity; normal elastic strain on the X, Y, and Z axes; elastic shear strain in the XY, YZ, and XZ planes; total equivalent strain; equivalent stress; maximum principal stress; minimum principal stress; maximum shear stress; normal stress on the X, Y, and Z axes; shear stress in the XY, YZ, and XZ planes.

The maximum, minimum, and mean values of the stress and strain are summarized in Figures 3–6 and Table 3, with and without a shoulder finish line. In Table 3 the values obtained from the FEA are summarized for all 3 directions for each model, namely A and B.

Table 3. Finite element results for total and directional (X, Y, Z) deformations for premolar FEA models under 200 N: A—shoulder finish line; B—no shoulder.

Characteristic	Total Deformation	Deformation *X* Axis	Deformation *Y* Axis	Deformation *Z* Axis
Model A—premolar prepared with shoulder finish line				
Minimum	0 mm	-6.95×10^{-5} mm	-5.26×10^{-4} mm	-1.11×10^{-3} mm
Maximum	1.17×10^{-3} mm	4.07×10^{-4} mm	5.76×10^{-5} mm	2.91×10^{-5} mm
Model B—premolar prepared with shoulder finish line				
Minimum	0 mm	-1.51×10^{-3} mm	-5.51×10^{-4} mm	-1.91×10^{-3} mm
Maximum	3.3×10^{-3} mm	4.31×10^{-4} mm	2.87×10^{-3} mm	5.45×10^{-4} mm

The highest total deformation for model A was recorded at the intercuspidal groove, whereas for model B it was located at the tip of the buccal cusp (Figure 3 and Table 3). For model A, the highest total deformation was recorded at the intercuspidal groove, while for model B it was observed at the tip of the vestibular cusp. In model A, the lowest total deformation was noted in the cervical area toward the oral side, whereas for model B it was recorded in the apical third of the tooth, also toward the oral side. For both models A and B, the minimum total deformation occurred at the abutment level, while the maximum values were found in the prosthetic reconstructions.

Deformation along the *X* axis (Figure 4 and Table 3) ranged for model A from a minimum value recorded at the level of the ledge to a maximum value recorded on the occlusal slope of the buccal cusp, with a corresponding average value. For model B, deformation along the *X* axis ranged from a minimum value recorded at the tip of the buccal cusp to a maximum value in the cervical area of the tooth, towards the oral side, with a corresponding average value. Both the maximum and minimum values occurred at the level of the prosthetic components.

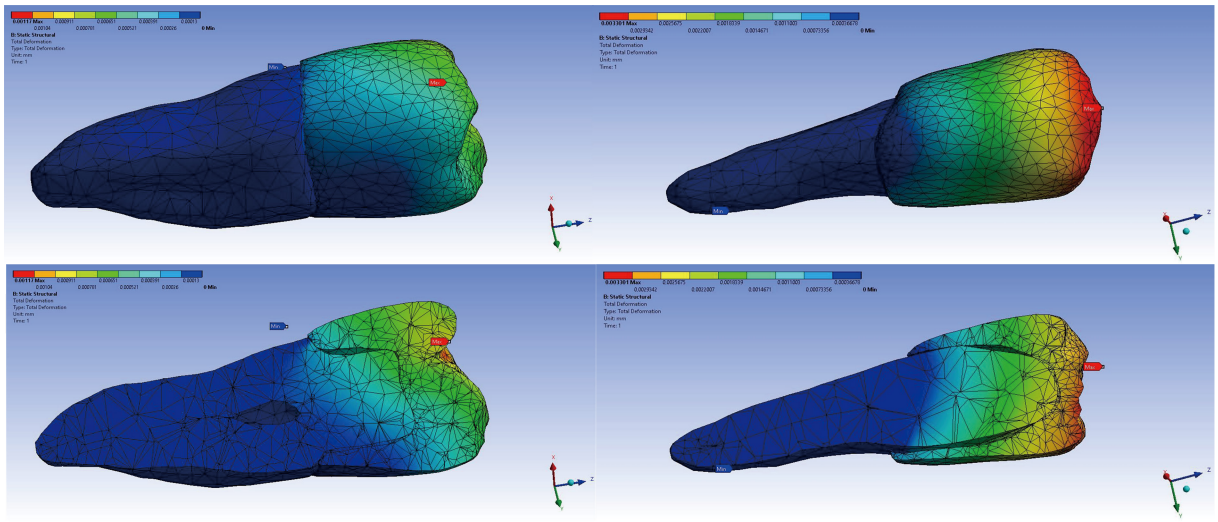


Figure 3. Total deformation for model A and model B.

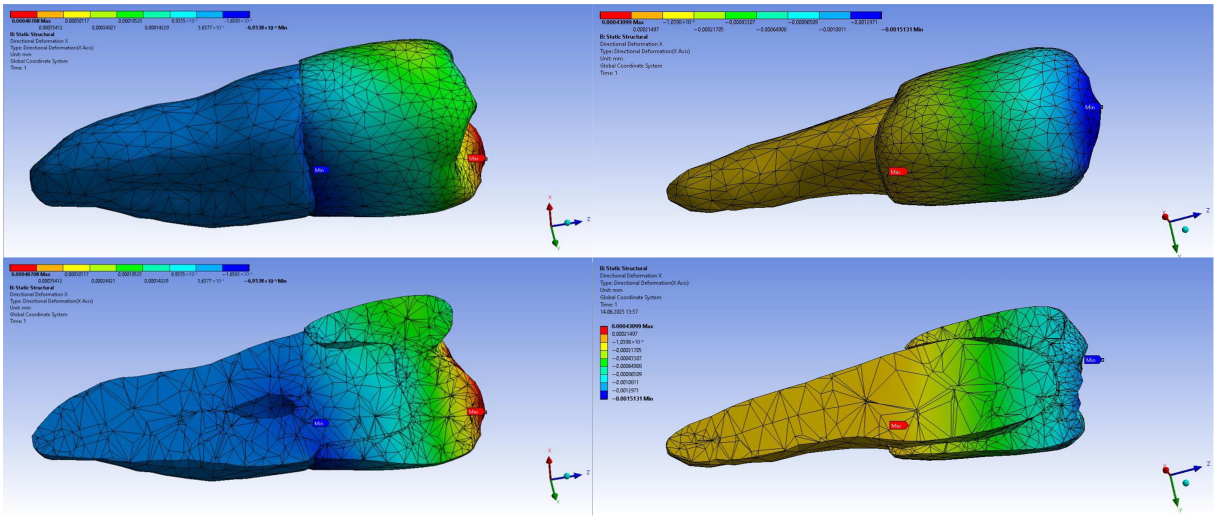


Figure 4. Deformation in the *X* axis for model A and model B.

Deformation along the *Y* axis (Figure 5 and Table 3) ranged for model A from a minimum value recorded on the occlusal slope of the oral cusp to a maximum value recorded at the ledge towards the oral side and on the buccal surface of the crown, with a corresponding average value. For model B, deformation along the *Y* axis ranged from a minimum value recorded in the cervical region towards the oral side to a maximum value at the tip of the buccal cusp, with a corresponding average value. Both the maximum and minimum values occurred at the level of the prosthetic components.

Deformation along the *Z* axis (Figure 6 and Table 3) ranged for model A from a minimum value recorded on the occlusal slope of the oral cusp to a maximum value recorded on the buccal surface of the crown, with a corresponding average value. For model B, the deformation along the *Z* axis ranged from a minimum value recorded on the oral slope of the oral cusp to a maximum value on the buccal surface of the crown, with a corresponding average value. Both the maximum and minimum values occurred at the level of the prosthetic components.

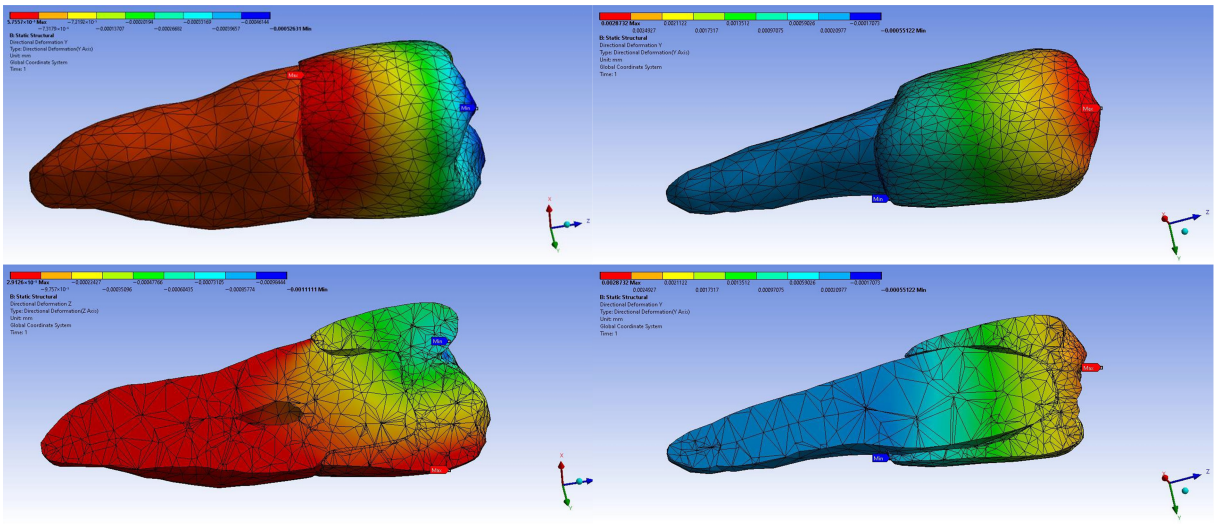


Figure 5. Deformation in the *Y* axis for model A and model B.

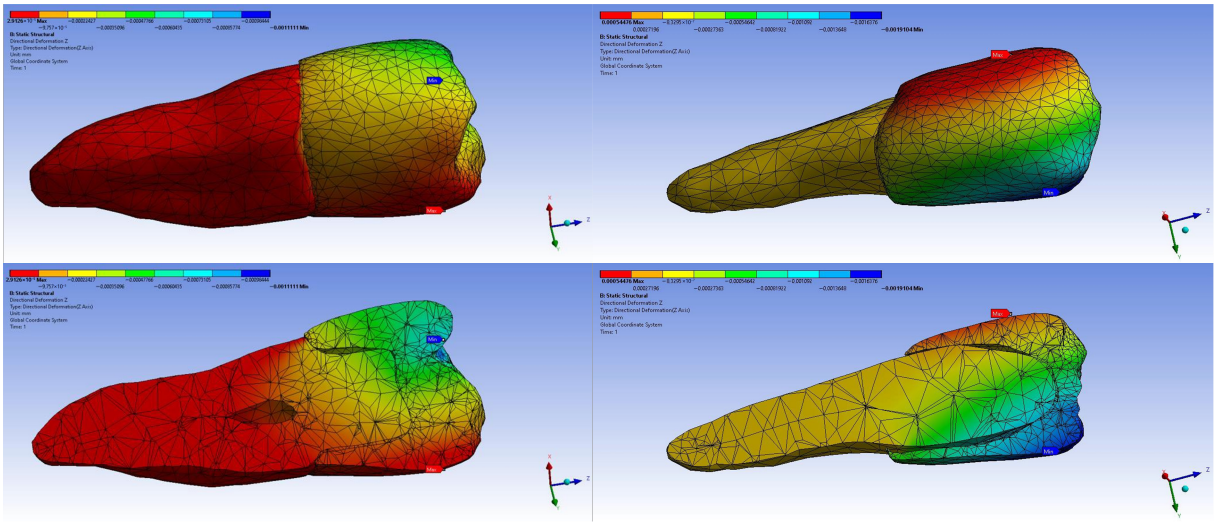


Figure 6. Deformation in the *Z* axis for model A and model B.

The equivalent stress (Figure 7 and Table 4) varied for model A between a value recorded at the apex and a value recorded at the ledge, towards the oral side, with an average of 7.73 MPa. For model B, it varied between a value recorded at the apex and 346 MPa (recorded at the cervical area, towards the oral side), with an average of 13.6 MPa. For both model A and model B, the minimum value was recorded on the abutments, and the maximum value on the prosthetic components.

Table 4. Minimum and maximum normal stresses (MPa) along the X, Y, and Z axes for two premolar FEA models. Under a 200 N vertical load (Z-axis).

Characteristic	Normal Stress X	Normal Stress Y	Normal Stress Z	Maximum Principal Stress	Minimum Principal Stress
Model A—premolar prepared with shoulder finish line					
Minimum	−74.6 MPa	−98.6 MPa	−243 MPa	−63.3 MPa	−248 MPa
Maximum	67.2 MPa	66.6 MPa	115 MPa	121 MPa	49.5 MPa
Model B—premolar prepared without shoulder finish line					
Minimum	−134 MPa	−161 MPa	−177 MPa	−76.7 MPa	−314 MPa
Maximum	102 MPa	76.4 MPa	273 MPa	320 MPa	15.4 MPa

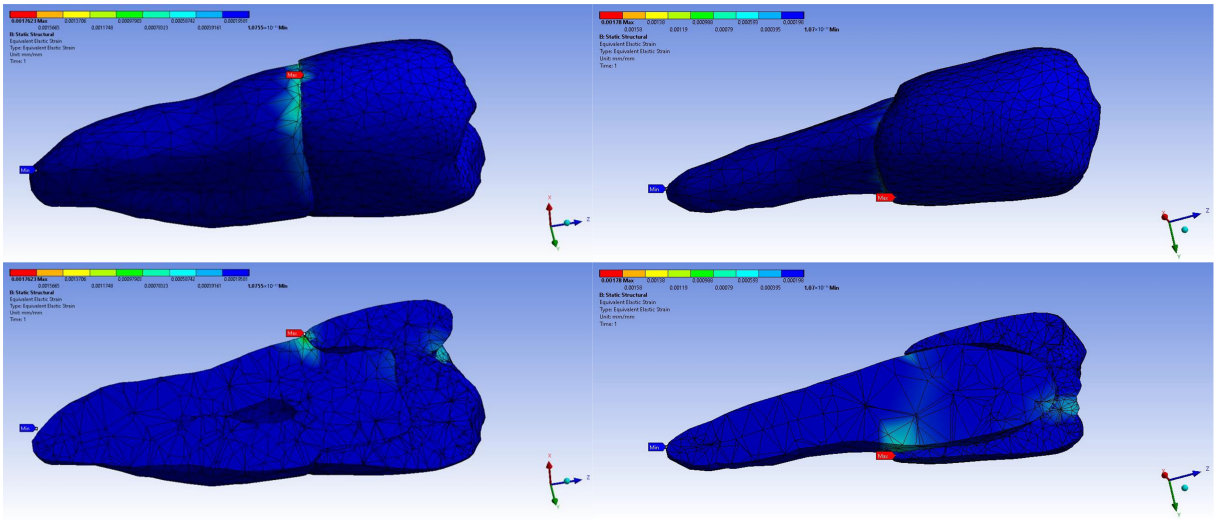


Figure 7. The equivalent stress when the experimental force is applied for model A and model B.

Table 4 presents the results of the equivalent stress along the X, Y, and Z axes for two premolar FEA models as well as the maximum and minimum stress.

The normal stress on the *X* axis (Figure 8 and Table 4) ranged for model A from −74.6 MPa (recorded at the ledge, towards the mesial side) to 67.2 MPa (recorded at the ledge, towards the oral side). For model B, it ranged from −134 MPa to 102 MPa (both values recorded at the cervical area, towards the oral side). In both cases, the maximum and minimum values occurred on the prosthetic components.

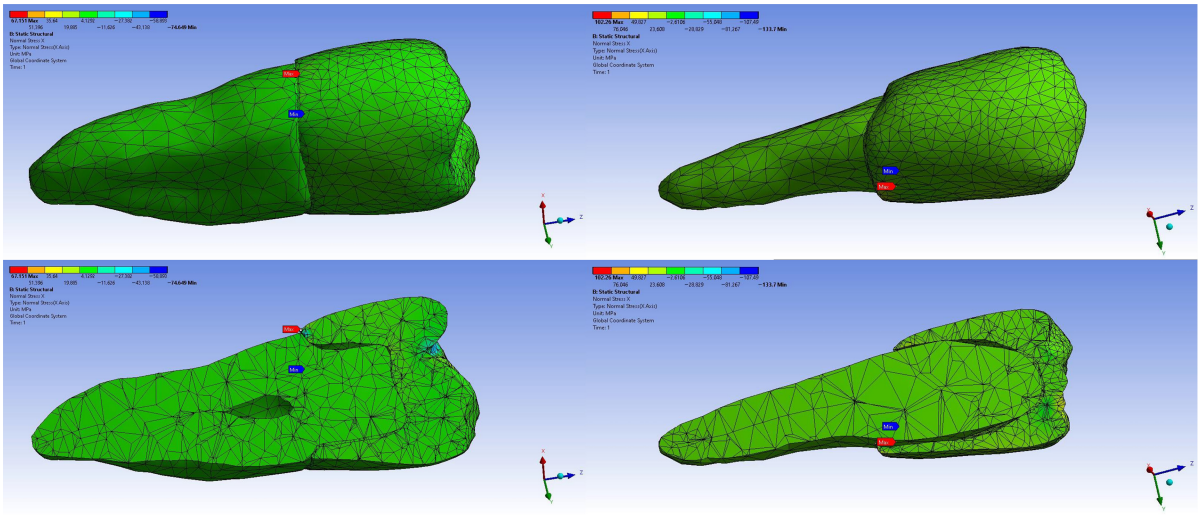


Figure 8. Localizations of normal stress *X* axis for model A and model B.

The normal stress on the *Y* axis (Figure 9 and Table 4) ranged for model A from −98.6 MPa (recorded on the occlusal slope of the oral cusp) to 66.6 MPa (recorded at the ledge, towards the oral side). For model B, it ranged from −161 MPa to 76.4 MPa (both values recorded at the cervical area, towards the oral side). In both cases, the maximum and minimum values occurred on the prosthetic components.

The normal stress on the *Z* axis (Figure 10 and Table 4) ranged for model A from −243 MPa to 115 MPa (both values recorded at the ledge, towards the oral side). For model B, it ranged from −177 MPa (recorded on the occlusal surface of the abutment) to 273 MPa (at the cervical area, towards the oral side). In both cases, the maximum and minimum values occurred on the prosthetic components.

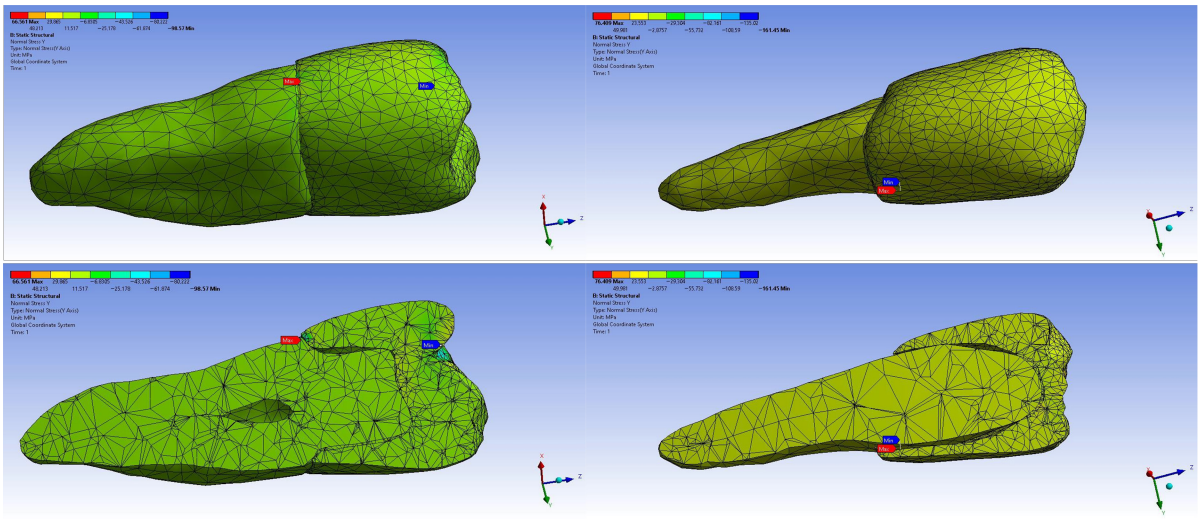


Figure 9. Localizations of normal stress *Y* axis for model A and model B.

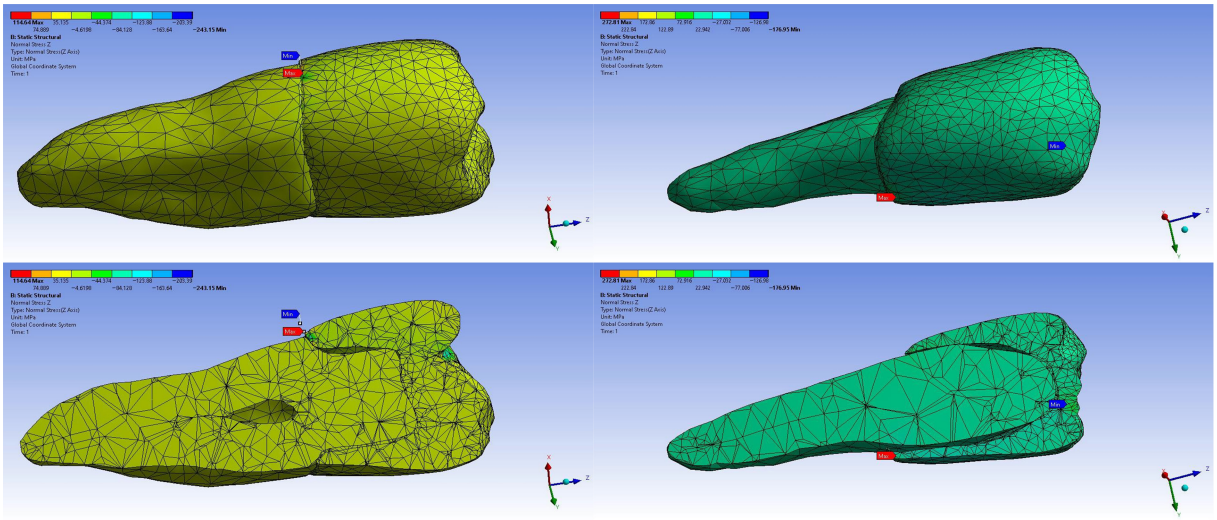


Figure 10. Localizations of normal stress *Z* axis for model A and model B.

The maximum principal stress (Figure 11 and Table 4) ranged for model A from a minimum value recorded on the occlusal slope of the oral cusp to a maximum value recorded at the ledge, towards the oral side, with a corresponding average value. For model B, it ranged from a minimum value recorded in the occlusal region of the abutment to a maximum value recorded at the cervical area, towards the oral side, with a corresponding average value. In both cases, the maximum and minimum values occurred on the prosthetic components.

The minimum principal stress (Figure 12 and Table 4) ranged for model A from a minimum value recorded at the ledge, towards the oral side, to a maximum value also recorded at the same level, towards the oral side, with a corresponding average value. For model B, it varied between a minimum and a maximum value, both recorded at the cervical area, towards the oral side, with a corresponding average value. In both cases, the maximum and minimum values occurred on the prosthetic components.

The figures for maximum principal elastic strain (Figure 13), minimum principal elastic strain (Figure 14), normal elastic strain along the *X* axis (Figure 15), normal elastic strain along the *Y* axis (Figure 16), normal elastic strain along the *Z* axis (Figure 17), and shear elastic strain in the XY plane (Figure 18), YZ plane (Figure 19), and XZ plane (Figure 20) show the maximum and minimum values recorded both on the prosthetic components and on the abutments. Furthermore, the obtained values are presented in Table 5.

Table 5. Summary of minimum and maximum values for elastic strain intensity, minimum principal elastic strain, normal elastic strains (X, Y, Z), and shear elastic strains (XY, YZ, XZ) in two premolar FEA models.

Characteristics	Elastic Strain Intensity	Minimum Principal Elastic Strain	Normal Elastic Strain X	Normal Elastic Strain Y	Normal Elastic Strain Z	Shear Elastic Strain XY	Shear Elastic Strain YZ	Shear Elastic Strain XZ
Model A—premolar prepared with shoulder finish line								
Minimum	6.09×10^{-12} mm/mm	-1.67×10^{-3} mm/mm	-1.65×10^{-4} mm/mm	-2.97×10^{-4} mm/mm	-1.42×10^{-3} mm/mm	-4.85×10^{-42} mm/mm	-2.14×10^{-3} mm/mm	-8.59×10^{-4} mm/mm
Maximum	2.56×10^{-3} mm/mm	-1.38×10^{-7} mm/mm	3.15×10^{-4} mm/mm	3.11×10^{-4} mm/mm	4.65×10^{-4} mm/mm	5.16×10^{-4} mm/mm	6.73×10^{-3} mm/mm	1.35×10^{-3} mm/mm
Model B—premolar prepared without shoulder finish line								
Minimum	1.49×10^{-11} mm/mm	-1.37×10^{-3} mm/mm	-7.06×10^{-4} mm/mm	-6.24×10^{-4} mm/mm	-7.54×10^{-4} mm/mm	-5.3×10^{-4} mm/mm	-1.76×10^{-3} mm/mm	-7.88×10^{-4} mm/mm
Maximum	2.37×10^{-3} mm/mm	-2.74×10^{-12} mm/mm	4.49×10^{-4} mm/mm	3.98×10^{-4} mm/mm	1.29×10^{-3} mm/mm	7.2×10^{-4} mm/mm	1.24×10^{-3} mm/mm	1.21×10^{-3} mm/mm

https://doi.org/10.3390/coatings16040482

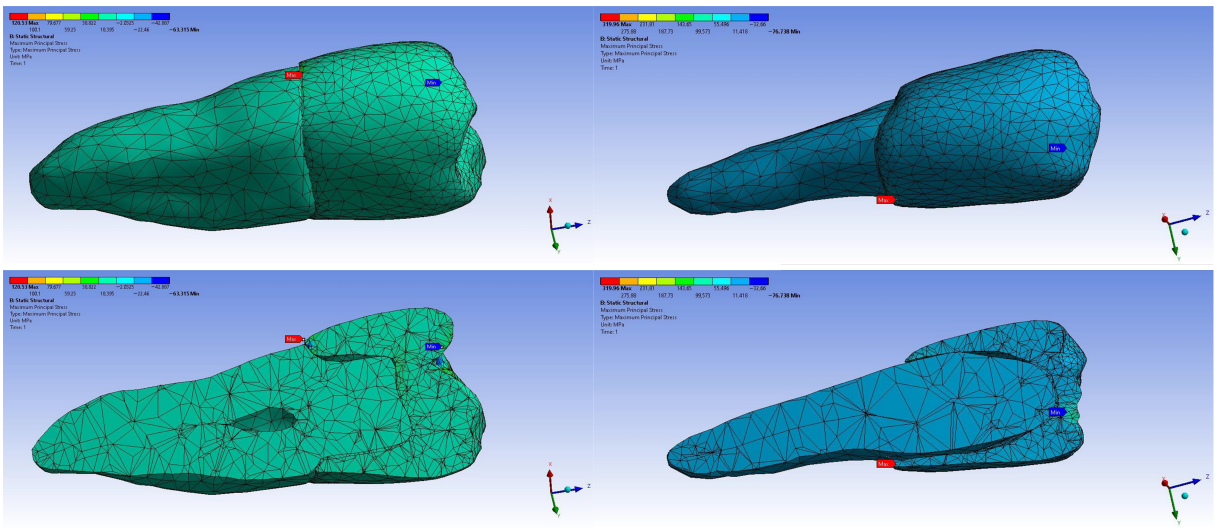


Figure 11. Maximum principal stress for model A and model B.

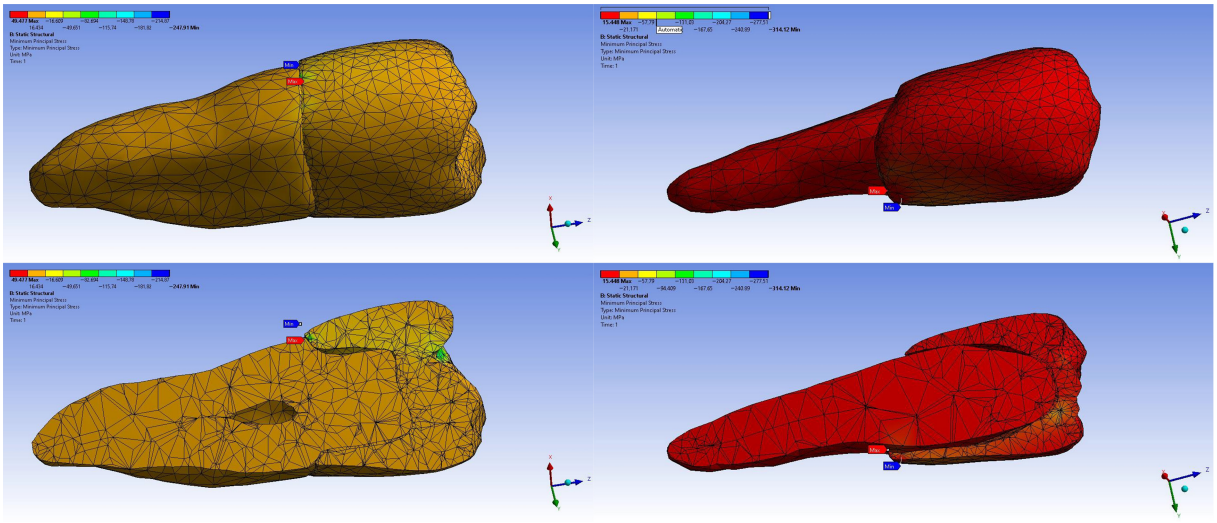


Figure 12. Minimum principal stress for model A and model B.

The maximum principal elastic strain (Figure 13) varied for model A and was recorded at the cervical margin toward the mesial aspect. For model B, the maximum principal strain also varied and was observed at the dental apex and at the cervical area toward the oral side. The highest values were recorded in the prosthetic components, while the lowest values were found at the abutments.

The minimum principal elastic strain (Figure 14) varied for model A, with values recorded at the cervical margin toward the oral side and at the mid-root level. For model B, the minimum principal elastic strain also varied, with values observed at the cervical area toward the oral side and at the apex. The highest values were recorded at the abutments, while the lowest values were found in the prosthetic components.

The normal elastic strain along the *X* axis (Figure 15) ranged for model A from -1.65×10^{-4} mm/mm (recorded at the ledge, towards the mesial side) to 3.15×10^{-4} mm/mm (recorded at the ledge, towards the oral side). For model B, it ranged from -7.06×10^{-4} mm/mm to 4.49×10^{-4} mm/mm (both values recorded in the vicinity of the cervical area, towards the oral side). In both cases, the maximum and minimum values occurred on the prosthetic components.

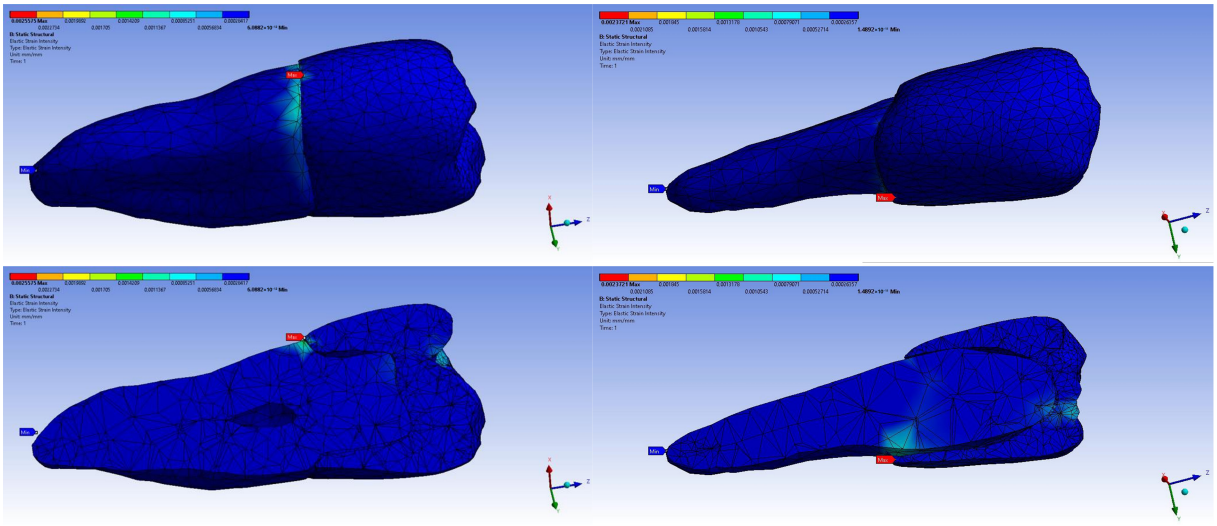


Figure 13. Maximum principle elastic strain for model A and model B after the application of an experimental force to the occlusal surface.

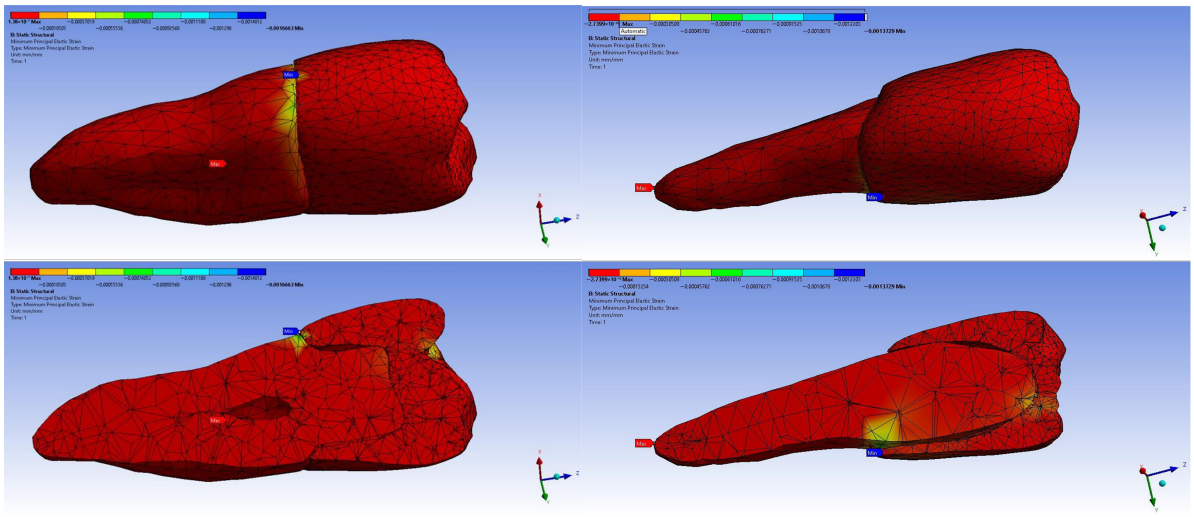


Figure 14. Minimum principal elastic strain for model A and model B after the application of an experimental force to the occlusal surface.

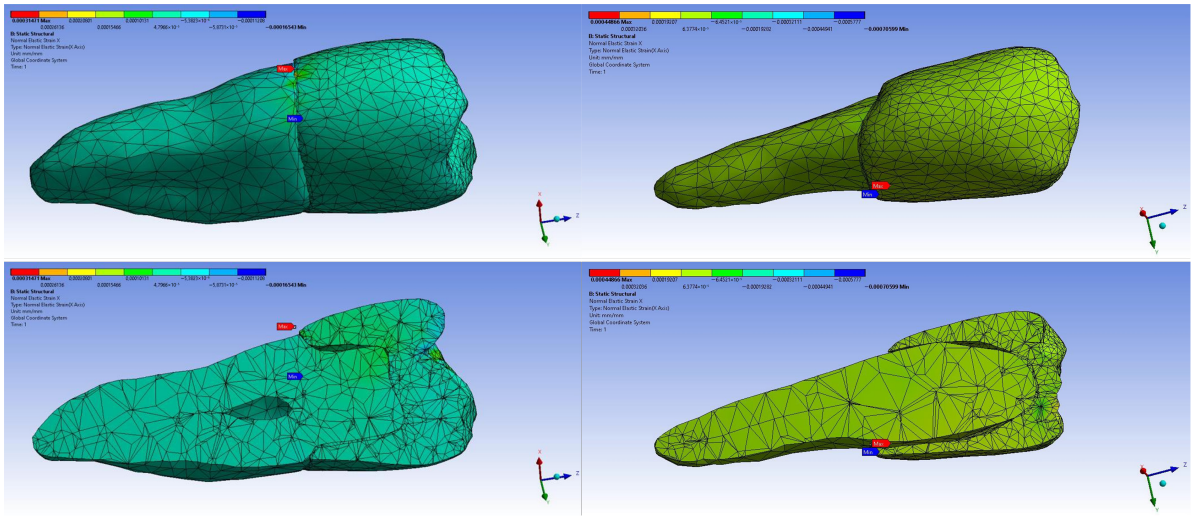


Figure 15. The normal elastic strain along the *X* axis for model A and model B after the application of an experimental force to the occlusal surface.

The normal elastic strain along the *Y* axis (Figure 16) ranged for model A from -2.97×10^{-4} mm/mm (recorded at the ledge, towards the mesial side) to 3.11×10^{-4} mm/mm (recorded at the ledge, towards the oral side). For model B, it ranged from -6.24×10^{-4} mm/mm to 3.98×10^{-4} mm/mm (both values recorded in the vicinity of the cervical area, towards the oral side). In both cases, the maximum and minimum values occurred on the prosthetic components.

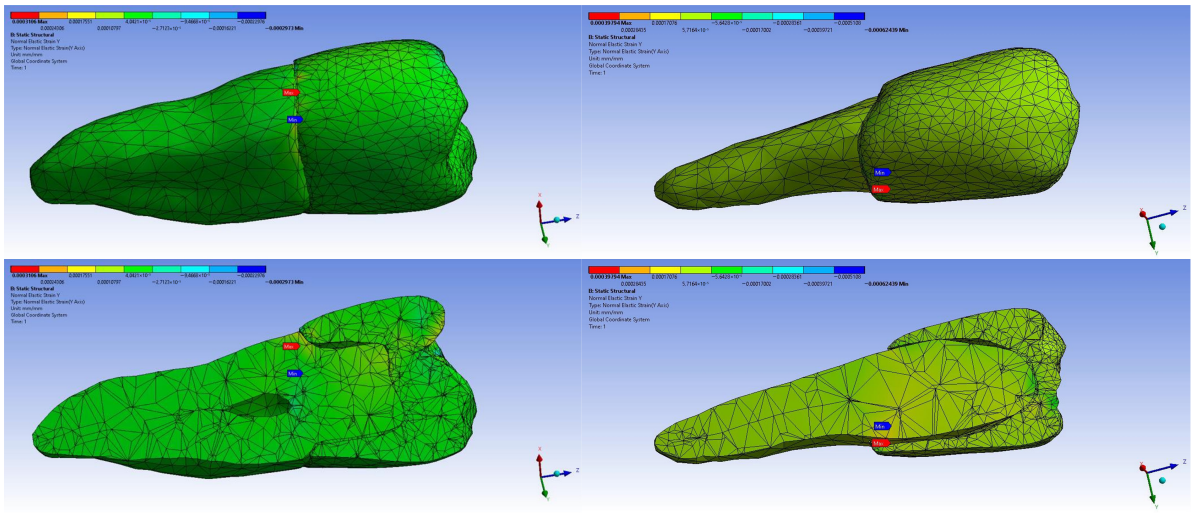


Figure 16. The normal elastic strain along the *Y* axis for model A and model B after the application of an experimental force to the occlusal surface.

The normal elastic strain along the *Z* axis (Figure 17) ranged for model A from -1.42×10^{-3} mm/mm to 4.65×10^{-4} mm/mm (both recorded at the ledge, towards the oral side). For model B, it ranged from -7.54×10^{-4} mm/mm to 1.29×10^{-3} mm/mm (both values recorded in the vicinity of the cervical area, towards the oral side). The maximum values were recorded on the prosthetic components, while the minimum values were recorded on the abutments.

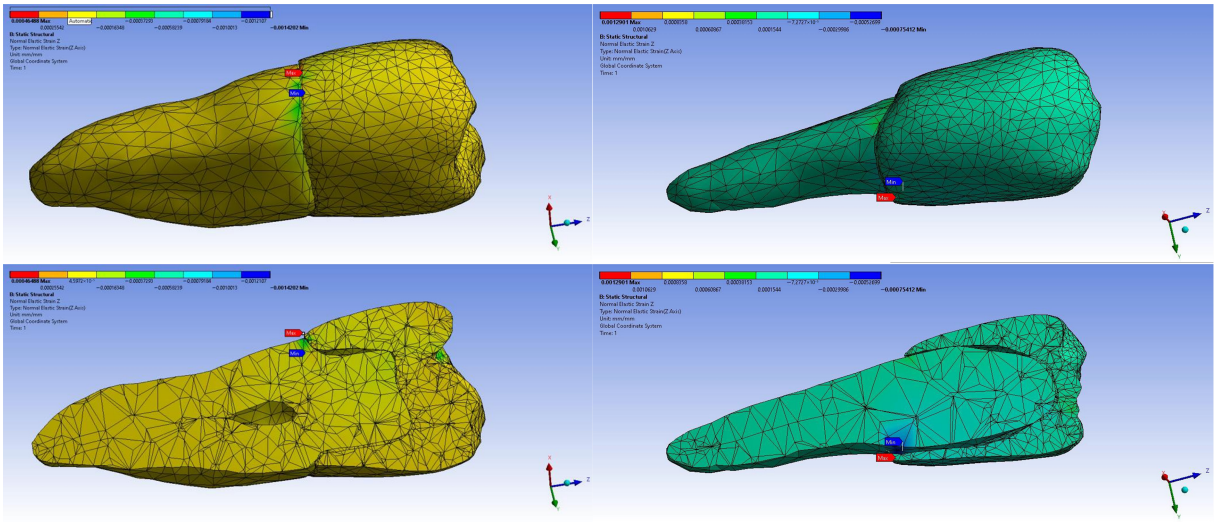


Figure 17. The normal elastic strain along the *Z* axis for model A and model B after the application of an experimental force to the occlusal surface.

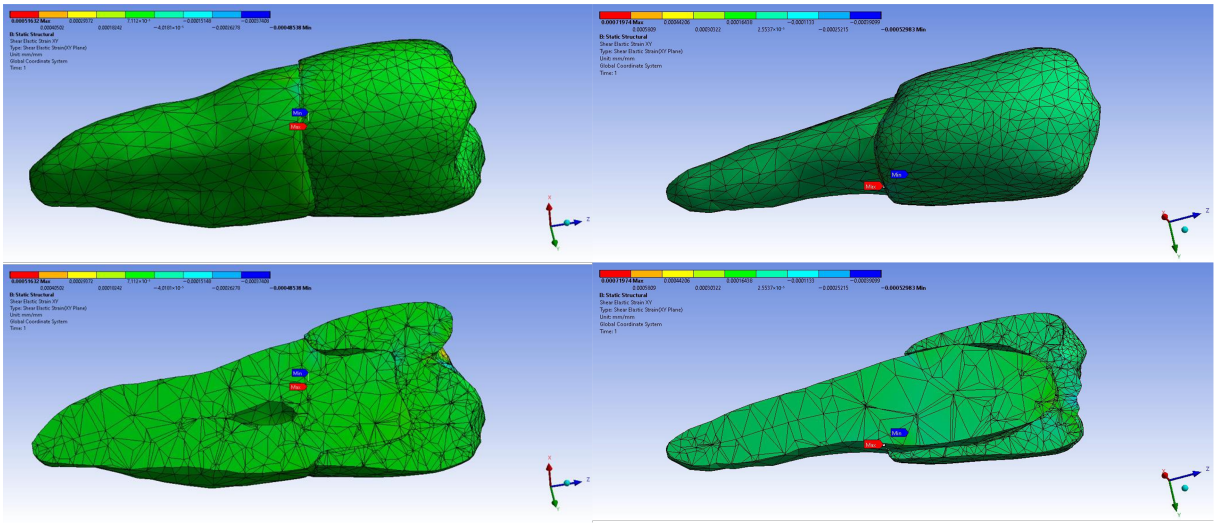


Figure 18. Shear elastic strain in the XY plane for model A and model B after the application of an experimental force to the occlusal surface.

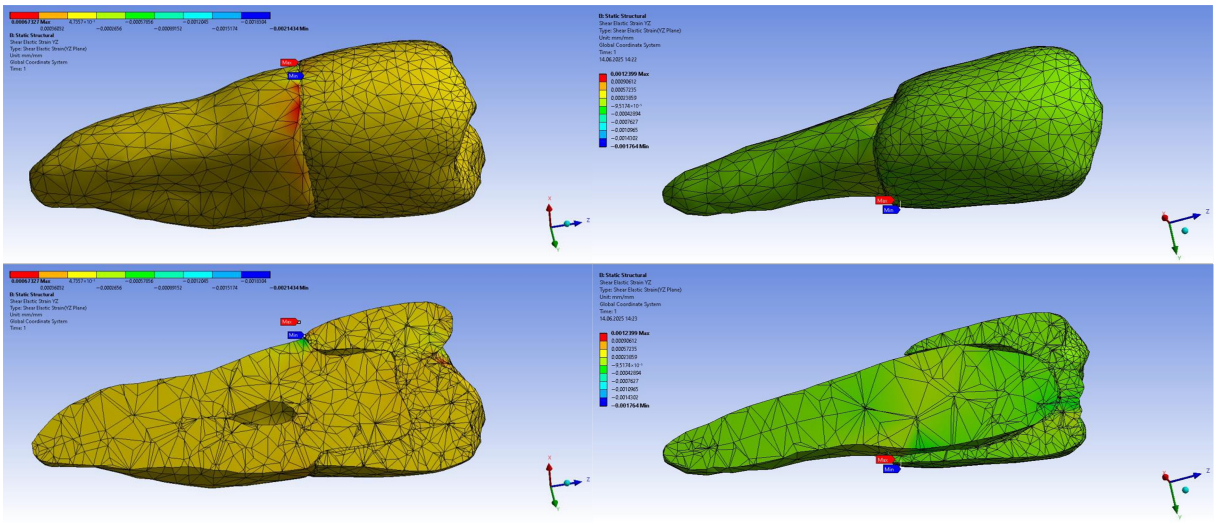


Figure 19. Shear elastic stain in the YZ plane for model A and model B after the application of an experimental force to the occlusal surface.

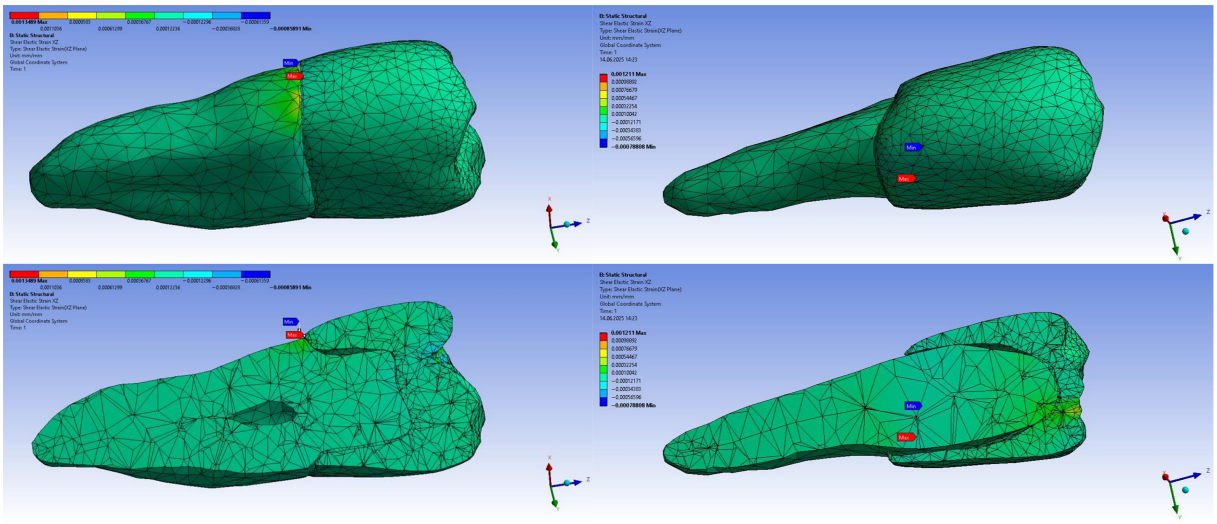


Figure 20. Shear elastic stain in the XZ plane for model A and model B after the application of an experimental force to the occlusal surface.

The maximum shear stress (Figure 21 and Table 6) varied for model A, with values recorded at the apex and at the cervical margin toward the oral side. For model B, variable values were recorded at the apex and at the cervical area toward the oral side. For both model A and model B, the minimum values were found at the abutments, while the maximum values were observed in the prosthetic components.

Table 6. Summary of minimum and maximum shear stress and equivalent (von Mises) stress (MPa) computed by FEA for two premolar models.

Characteristics	Maximum Shear Stress	Equivalent Stress
Model A—premolar prepared with shoulder finish line		
Minimum	4.21×10^{-8} MPa	7.6×10^{-8} MPa
Maximum	101 MPa	182 MPa
Model B—premolar prepared without shoulder finish line		
Minimum	1.43×10^{-7} MPa	2.65×10^{-7} MPa
Maximum	187 MPa	346 MPa

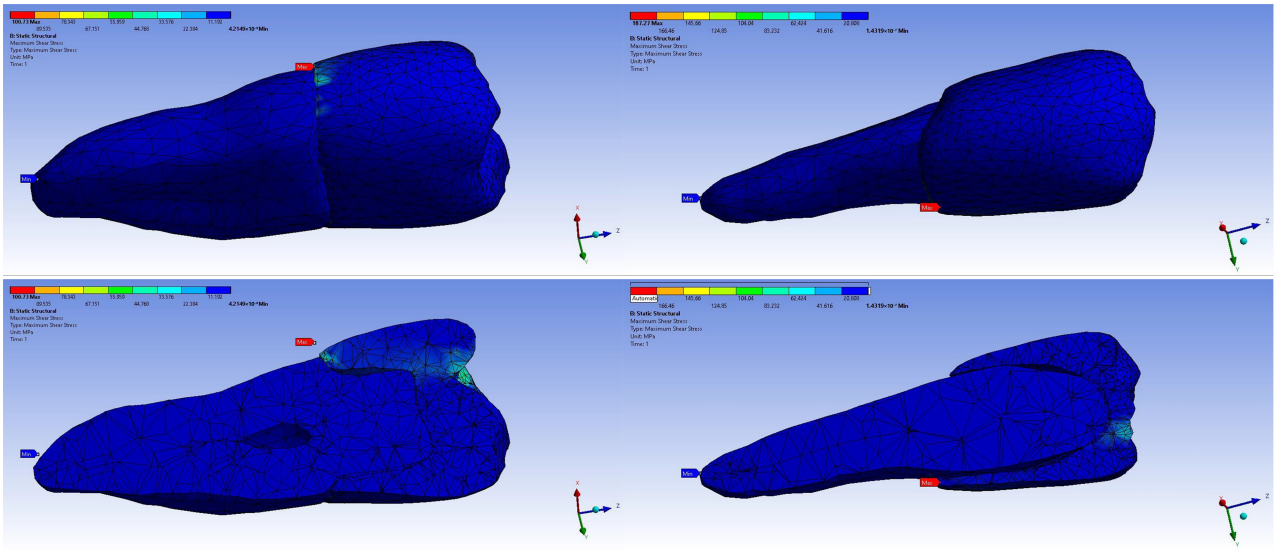


Figure 21. Maximum shear stress for model A and model B.

The equivalent stress (Figure 22 and Table 6) varied for model A, with values recorded at the apex and at the cervical margin toward the oral side. For model B, the values were recorded at the apex and at the cervical area toward the oral side. For both model A and model B, the minimum values were found at the abutments, while the maximum values were observed in the prosthetic components.

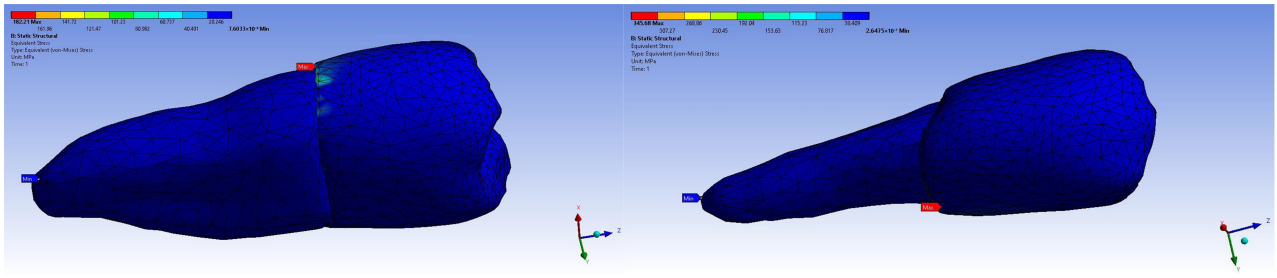


Figure 22. *Cont.*

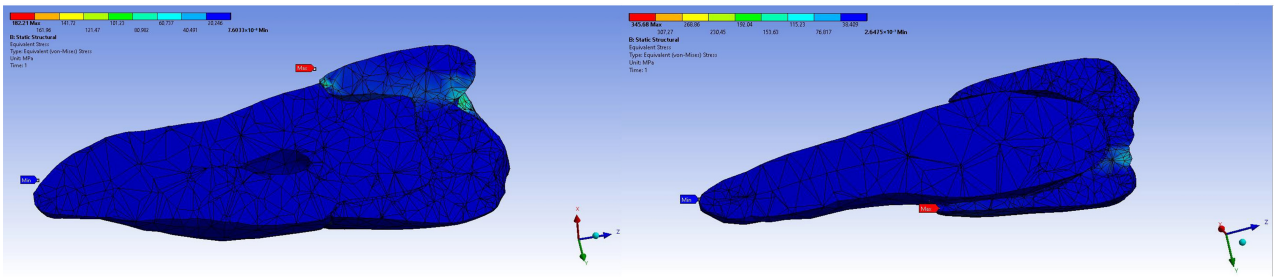


Figure 22. Equivalent stress for model A and model B.

An experimental force of 200 N was applied along the Z axis to both models—A (with a shoulder finish line) and B (without a shoulder finish line)—in accordance with the principles of functional occlusion. The analysis performed for each model revealed the development of significant deformations both at the level of the dental abutments and the prosthetic components.

4. Discussion

FEA played a crucial role in evaluating the behavior of each material under the action of mechanical forces. Zirconia demonstrated superior biomechanical performance, characterized by a uniform distribution of stress and high fracture resistance. Results showed zirconia ensures effective stress distribution in critical areas, thereby preventing deformation and localized stress concentration, which are essential for the long-term durability of restorations [12,18,19]. This is consistent with FEM studies on crowns reporting favorable von Mises stress distribution and lower peak stress for zirconia compared with several alternative materials under axial loading [20–22].

The present study focuses on the modifications exhibited by zirconia crowns in the premolar region under experimental forces of 200 N and in relation to the type of preparation. However, there are studies that consider that prior to the implementation of a new type of prosthetic restoration or material in clinical practice, its mechanical behavior must be assessed through preclinical tests.

Similar finite element assessments of CAD/CAM-fabricated ceramic dowels have demonstrated that custom design strongly influences stress distribution and fracture resistance. This underscores the necessity for meticulous preclinical evaluation of novel restorative solutions [23]. Moreover, marginal and/or morphological design can modulate occlusal stress patterns. Three-dimensional (3D) FEA of occlusal restorations shows that different margin configurations measurably alter stress magnitudes in both the restoration and tooth substrate [24]. A restoration is considered suitable for use if its fracture resistance exceeds the estimated maximum occlusal force, which, in the molar region, is approximately 500 N [18].

In the context of preparation design and prosthetic longevity, it is important to note that the vertical edgeless preparation—also known as the biologically oriented preparation technique (BOPT) or vertical edgeless preparation (VEP)—is generally regarded as a conservative approach. This technique eliminates a distinct finish line and is widely employed in clinical practice, particularly for teeth with compromised periodontal support or when maximal preservation of tooth structure is desired. In this method, the preparation is placed subgingivally, typically up to the level of the epithelial attachment, allowing for soft-tissue healing that reestablishes a mucosal profile and conceals the tooth–restoration junction. The resulting “edgeless” margin lacks pronounced internal angles or visible contours. In contrast, the gingival threshold (horizontal shoulder finish line) is prepared using cylindrical or cylindrical–conical, flat-ended diamond instruments to create a horizontal platform

approximately perpendicular (≈90°) to the long axis of the tooth. This design is generally indicated when dental tissues are intact and prosthetic stability is not compromised.

It is essential to acknowledge the limitations inherent in the present study concerning finite element analysis (FEA), particularly due to the idealizations involved in this type of analysis. Specifically, the geometry was reconstructed from computed tomography (CT) scans and subsequently simplified for meshing, which did not fully account for the interpatient variability in tooth anatomy. Furthermore, the materials were modeled as linear elastic, homogeneous, and isotropic, with Young's modulus and Poisson's ratio selected from established literature ranges.

This methodology introduces parameter uncertainty; however, the same assumptions were consistently applied across groups to ensure the validity of relative comparisons. To simulate a definitive restoration that is fixed and cemented, the crown and abutment were modeled as perfectly bonded, with no slip or separation. The periodontal ligament and the cement layer were omitted, thereby focusing the model on load transfer at the intimate contact. Nonetheless, this approach may underestimate the compliance of supporting tissues and interfacial effects.

The crowns were virtually positioned in Mimics rather than being physically manufactured, thus manufacturing tolerances and variability in cement thickness were not represented. These idealizations may affect the absolute values of stress and strain, yet the spatial distributions and comparative trends between preparations are anticipated to remain robust. Under the experimental conditions applied, no indications of stress shielding were detected.

Thus, even within its limitation, FEA has been shown to decrease the number of laboratory experiments and to support a more cost-effective development of dental prostheses [25]. Beyond restorative dentistry, finite element analysis has also been successfully applied in orthodontics, where studies on fixed functional appliances demonstrated its utility in predicting maxillary stress changes under complex loading [26].

FEA and modeling have brought significant advances in dental biomechanics, allowing 3D replication of most dental structures, which differ in shape and loading mode [27]. FEA is an efficient method for investigating and analyzing complex structures, which are difficult to standardize in vitro and in vivo studies [28]. In zirconia specifically, refined numerical approaches (e.g., homogenization-based modeling) have been used to characterize stress and displacement fields at clinically relevant geometries [25].

A complex study regarding fracture resistance for convergent occlusal areas of implant abutments using FEA demonstrated that thicker zirconia specimens presented higher fracture resistance and the lowest stress values under a 300 N load [29]. Additional FEM investigations on implant-supported abutments, such as OT Bridge systems with Seeger retention, confirm that abutment design plays a critical role in stress concentration and long-term biomechanical behavior [30]. Comparative FEA on fixed partial dentures similarly demonstrates lower or more favorably distributed stress in zirconia frameworks versus lithium-disilicate glass-ceramics or gold alloy, supporting zirconia selection where occlusal demands are higher [31,32].

Zirconia continues to be the material of choice for restorations exposed to high occlusal forces, due to its excellent fracture resistance and its ability to provide a uniform distribution of stress [12]. Nonetheless, thermomechanical fatigue and interfacial integrity influence longevity in all-ceramic systems, with cyclic loading and thermal aging reducing bond strength; this highlights the importance of cementation and aging protocols when interpreting FEA outcomes [33]. In cases of failure, FEA indicates that specific repair strategies for monolithic zirconia can partially restore favorable stress profiles, offering a biomechanically rational alternative to full replacement [34].

Although time-consuming FEA is considered by many authors to be a valuable tool for explaining the occurrence of a series of unwanted phenomena at the level of some teeth, implants, direct or indirect restorations, and the dental materials used, and can indicate the vulnerable areas where maximum stress and deformations are developed [35–40].

In this light it must be highlighted that future work will include explicit models of the periodontal ligament and the cement layer and will perform sensitivity analyses on elastic constants and interface behavior using a cohesive contact formulation.

5. Conclusions

This study provided a detailed analysis of the biomechanical behavior of zirconia crowns cemented onto tooth abutments prepared with or without a shoulder finish line, using finite element analysis. The results obtained, correlated with data from the literature, led to the following conclusions:

- Zirconia crowns were subjected to greater stress than the tooth abutments, regardless of the type of preparation. Thus, out of 25 simulations performed for each of model A and model B regarding the stresses and strains developed, in 16 simulations both the minimum and maximum loads appeared at the crowns, in 8 cases the minimum loads appeared at the abutments and the maximum loads at the crowns, and only in a single case, that of the minimum principal elastic strain, the maximum value appeared on the abutments and the minimum on the prosthetic restorations.
- According to the simulations carried out, the preparation with a shoulder finish line (A) demonstrated better biomechanical behavior. Thus, out of 25 mechanical tests performed for each model A and model B regarding the stresses and strains developed, in two cases the recorded values were very close, in 4 cases the recorded values were higher for model A, and in 19 cases the recorded values were higher for model B.
- In clinical practice, it is advised that when sufficient coronal structure and periodontal conditions permit supra- or equigingival margins, a shoulder finish line may more effectively mitigate mechanical stress. Conversely, vertical edgeless margins are considered appropriate in scenarios where tissue preservation or compromised support is a primary concern. This approach, however, necessitates precise management of cervical contouring and occlusal load.

While acknowledging its limitations, this study offers a deeper insight into the impact of preparation design on the biomechanical properties of dental restorations, with a particular focus on zirconia-based restorations. The results of this research provide essential guidance for selecting the most suitable clinical strategies for prosthetic preparation techniques.

Author Contributions: Conceptualization, L.A.D., M.T. and R.M.C.; methodology, Ș.E.C.-C. and A.M.P.; investigation, A.C., M.V.C. and M.R.C.; writing—original draft preparation, L.A.D. and R.M.C.; data curation, M.T.; writing—review and editing, L.L.M., Ș.E.C.-C., A.C., A.M.P., M.V.C. and M.R.C.; design L.L.M. All authors have read and agreed to the published version of the manuscript.

Funding: This research received no external funding.

Institutional Review Board Statement: The protocol was authorized by Ethics Committee of the Faculty of Dental Medicine , Titu Maiorescu University of Bucharest (No.2 of 15 January 2024).

Informed Consent Statement: Informed consent was obtained from all subjects involved in the study.Written informed consent has been obtained from the patients to publish this paper.

Data Availability Statement: The present study's data are available with the corresponding author on request.

Conflicts of Interest: The authors declare no conflicts of interest.

Abbreviations

FEA	Finite Element Analysis
FEM	Finite Element Method
3D	Three-Dimensional
CAD/CAM	Computer-Aided Design/Computer-Aided Manufacturing
CT	Computed Tomography
STL	Standard Tessellation Language (or Standard Triangle Language)
OT	Overdenture Telescopic (in OT Bridge System)

References

1. Choi, A.H.; Conway, R.C.; Ben-Nissan, B. Finite-element modeling and analysis in nanomedicine and dentistry. *Nanomedicine* **2014**, *9*, 1681–1695. [CrossRef]
2. Xie, B.; Zhang, L.; Wang, Y.; Chu, Y.; Lu, Y. Finite element analysis in the dental sciences: A bibliometric and a visual study. *Int. Dent. J.* **2025**, *75*, 855–867. [CrossRef] [PubMed]
3. Carpegna, G.; Alovisi, M.; Paolino, D.S.; Marchetti, A.; Gibello, U.; Scotti, N.; Pasqualini, D.; Scattina, A.; Chiandussi, G.; Berutti, E. Evaluation of pressure distribution against root canal walls of NiTi rotary instruments by finite element analysis. *Appl. Sci.* **2020**, *10*, 2981. [CrossRef]
4. Viceconti, M.; Olsen, S.; Nolte, L.P.; Burton, K. Extracting clinically relevant data from finite element simulations. *Clin. Biomech.* **2005**, *20*, 451–454. [CrossRef] [PubMed]
5. Shayanfard, P.; Tan, X.; Karl, M.; Wendler, F. Finite element combined design and material optimization addressing the wear in removable implant prosthodontics. *J. Funct. Biomater.* **2024**, *15*, 344. [CrossRef]
6. Coman, C.; Ghergic, D.L.; Patroi, D.N.; Tarcolea, M.; Comăneanu, R.M.; Barbu, H.M. Comparative Assessment of Resistance Against Experimental Forces of Mixed Prosthetic Restorations. *Mater. Plast.* **2016**, *53*, 91–94.
7. Beresescu, G.; Ormenişan, A.; Comăneanu, R.M.; Carp Veliscu, A.M.; Manea, M.M.; Ion, R. FEM Analysis of Stress in Non-Carious Cervical Lesion Restoration with Four Different Restorative Materials. *Mater. Plast.* **2018**, *55*, 42–45. [CrossRef]
8. Coşarcă, A.S.; Grigoraş, R.; Hancu, V.; Coman, C.; Comăneanu, R.M.; Moraru, L.; Târcolea, M.; Ormenişan, A. Estimation by FEA of Mandibular Bone Strength Affected by the Presence of Benign Tumors Associated with Impacted Teeth. *Mater. Plast.* **2016**, *53*, 135–138.
9. Drăguş, L.; Tinu, A.S.; Coman, C.; Comăneanu, R.M.; Ghergic, D.L. Preliminary Studies on the Biomechanical Behavior of Metal-Ceramic Restorations. *Rev. Chim.* **2018**, *69*, 2594–2596. [CrossRef]
10. Baggi, L.; Cappelloni, I.; Di Girolamo, M.; Maceri, F.; Vairo, G. The influence of implant diameter and length on stress distribution of osseointegrated implants related to crestal bone geometry: A three-dimensional finite element analysis. *J. Prosthet. Dent.* **2008**, *100*, 422–431. [CrossRef]
11. Cattaneo, P.M.; Dalstra, M.; Melsen, B. The finite element method: A tool to study orthodontic tooth movement. *J. Dent. Res.* **2005**, *84*, 428–433. [CrossRef]
12. Petrie, C.S.; Williams, J.L. Comparative evaluation of implant designs: Influence of diameter, length, and taper on strains in the alveolar crest—A three-dimensional finite-element analysis. *Clin. Oral Implants Res.* **2005**, *16*, 486–494. [CrossRef]
13. Di Francesco, P.; Bechir, A.; Popescu, A.I.; Chivu, M.V.; Dobrescu, A.M.; Comăneanu, R.M.; Târcolea, M. Finite element analysis (FEA) of the stress behavior of some dental materials. *J. Med. Life* **2025**, *18*, 29–37. [CrossRef]
14. Lahoud, P.; Faghihian, H.; Richert, R.; Jacobs, R.; EzEldeen, M. Finite element models: A road to in-silico modeling in the age of personalized dentistry. *J. Dent.* **2024**, *150*, 105348. [CrossRef]
15. Zupancic Cepic, L.; Frank, M.; Reisinger, A.; Pahr, D.; Zechner, W.; Schedle, A. Biomechanical finite element analysis of short-implant-supported, 3-unit, fixed CAD/CAM prostheses in the posterior mandible. *Int. J. Implant Dent.* **2022**, *8*, 8. [CrossRef]
16. Ceddia, M.; Lamberti, L.; Trentadue, B. FEA comparison of the mechanical behavior of three dental crown materials: Enamel, ceramic, and zirconia. *Materials* **2024**, *17*, 673. [CrossRef] [PubMed]
17. Sharanraj, V.; Ramesha, C.; Kumar, V.; Chandran, R.; Madhavan, S. Finite element analysis of zirconia ceramic biomaterials used in medical dental implants. *Interceram-Int. Ceram. Rev.* **2019**, *68*, 24–31. [CrossRef]
18. Waldecker, M.; Rues, S.; Rammelsberg, P.; Bömicke, W. Validation of in-vitro tests of zirconia-ceramic inlay-retained fixed partial dentures: A finite element analysis. *Dent. Mater.* **2019**, *35*, e53–e62. [CrossRef] [PubMed]
19. Tyagi, R.; Kumar, S.; Aggarwal, R.; Choudhary, S.; Malethia, A.; Saini, N. A 3-D finite element analysis of stress distribution on implant-supported fixed prosthesis with four different commercially available implant systems. *J. Contemp. Dent. Pract.* **2020**, *21*, 835–840. [CrossRef] [PubMed]

20. Bramanti, E.; Cervino, G.; Lauritano, F.; Fiorillo, L.; D'Amico, C.; Sambataro, S.; Denaro, D.; Famà, F.; Ierardo, G.; Polimeni, A.; et al. FEM and Von Mises analysis on prosthetic crowns structural elements: Evaluation of different applied materials. *Sci. World J.* **2017**, *2017*, 1029574. [CrossRef]
21. Dzięgielewski, M.; Regulska, K.; Korycki, R.; Klimek, L. Analysis of stress and displacement fields in prosthetic crowns made of zirconium dioxide using numerical approach of homogenization hypothesis. *Materials* **2022**, *15*, 7716. [CrossRef]
22. Dejak, B.; Młotkowski, A.; Langot, C. Three-dimensional finite element analysis of molars with thin-walled prosthetic crowns made of various materials. *Dent. Mater.* **2012**, *28*, 433–441. [CrossRef]
23. Marghalani, T.Y.; Hamed, M.T.; Awad, M.A.; Naguib, G.H.; Elragi, A.F. Three-dimensional finite element analysis of custom-made ceramic dowel made using CAD/CAM technology. *J. Prosthodont.* **2012**, *21*, 440–450. [CrossRef]
24. Chen, Q.; Luo, S.; Wang, Y.; Chen, Z.; Li, Y.; Meng, M.; Li, Y.; Xiao, N.; Dong, Q. Three-dimensional finite element analysis of occlusal stress on maxillary first molars with different marginal morphologies restored with occlusal veneers. *BMC Oral Health* **2024**, *24*, 1349. [CrossRef]
25. Hassan, O.; Hamza, T.; Mohammed, F.M. Influence of design and material on load bearing capacity of fixed dental prosthesis: A finite element analysis. *Al-Azhar J. Dent. Sci.* **2022**, *25*, 1343. [CrossRef]
26. Kendre, B.; Kumar, A.; Shetty, K.N.; Hedge, G.; Umale, V.; Kulshrestha, R. Evaluation of stress changes in the maxilla with fixed functional appliances—A 3D FEM study. *J. Orthod. Sci.* **2021**, *10*, 10. [CrossRef] [PubMed]
27. Modi, R.; Kohli, S.; Rajeshwari, K.; Bhatia, S. A three-dimensional finite element analysis to evaluate the stress distribution in tooth-supported 5-unit intermediate abutment prosthesis with rigid and nonrigid connector. *Eur. J. Dent.* **2015**, *9*, 255–261. [CrossRef]
28. Ajaj Al-Kordy, N.M.T.; Al-Saadi, M.H. Finite element study of stress distribution with tooth-supported mandibular overdenture retained by ball attachments or resilient telescopic crowns. *Eur. J. Dent.* **2023**, *17*, 539–547. [CrossRef]
29. Lan, T.-H.; Pan, C.-Y.; Liu, P.-H.; Chou, M.M.C. Fracture resistance of monolithic zirconia crowns on four occlusal convergent abutments in implant prosthesis. *Appl. Sci.* **2019**, *9*, 2585. [CrossRef]
30. Cervino, G.; Cicciù, M.; Fedi, S.; Milone, D.; Fiorillo, L. FEM analysis applied to OT bridge abutment with Seeger retention system. *Eur. J. Dent.* **2021**, *15*, 47–53. [CrossRef] [PubMed]
31. Zheng, Z.; Lin, J.; Shinya, A.; Matinlinna, J.P.; Botelho, M.G.; Shinya, A. Finite element analysis to compare stress distribution of gold alloy, lithium-disilicate reinforced glass ceramic and zirconia-based fixed partial denture. *J. Investig. Clin. Dent.* **2012**, *3*, 291–297. [CrossRef] [PubMed]
32. Cardelli, P.L.; Vertucci, V.; Balestra, F.; Montani, M.; Arcuri, C. Mechanical evaluation and FEM analysis of stress in fixed partial dentures zirconium-ceramic. *Oral Implantol.* **2014**, *6*, 55–62. [CrossRef]
33. Vidotti, H.A.; Pereira, J.R.; Insaurralde, E.; Plaça, L.F.; Delben, J.R.; do Valle, A.L. Influence of thermal and mechanical fatigue on the shear bond strength of different all-ceramic systems. *J. Clin. Exp. Dent.* **2017**, *9*, e952–e957. [CrossRef] [PubMed]
34. Soares, P.M.; da Rosa, L.S.; Pereira, G.K.R.; Valandro, L.F.; Rippe, M.P.; Dal Piva, A.M.O.; Feilzer, A.J.; Kleverlaan, C.J.; Tribst, J.P.M. Mechanical behavior of repaired monolithic crowns: A 3D finite element analysis. *Dent. J.* **2023**, *11*, 254. [CrossRef]
35. Alemayehu, D.B.; Jeng, Y.R. Three-Dimensional Finite Element Investigation into Effects of Implant Thread Design and Loading Rate on Stress Distribution in Dental Implants and Anisotropic Bone. *Materials* **2021**, *14*, 6974. [CrossRef]
36. Germán-Sandoval, R.; Ortiz-Magdaleno, M.; Sánchez-Robles, P.; Zavala-Alonso, N.; Fernando Romo-Ramírez, G. Analysis of the Mechanical Behavior and Effect of Cyclic Fatigue on the Implant-Abutment Interface. *Odovtos Int. J. Dent. Sci.* **2021**, *23*, 104–114. [CrossRef]
37. Nie, H.; Tang, Y.; Yang, Y.; Wu, W.; Zhou, W.; Liu, Z. Influence of a new abutment design concept on the biomechanics of peri-implant bone, implant components, and microgap formation: A finite element analysis. *BMC Oral Health* **2023**, *23*, 277. [CrossRef]
38. Comaneanu, R.M.; Mihali, T.; Gioga, C.; Pangica, A.-M.; Perlea, P.; Coman, C.; Hancu, V.; Botoaca, O.; Voiculeanu, M.; Tarcolea, M. FEA on the biomechanical behavior of immediately loaded implants with different sizes. *Rom. J. Stomatol.* **2023**, *69*, 116–122. [CrossRef]
39. Gönder, H.Y.; Mohammadi, R.; Harmankaya, A.; Yüksel, İ.B.; Fidancıoğlu, Y.D.; Karabekiroğlu, S. Teeth Restored with Bulk–Fill Composites and Conventional Resin Composites; Investigation of Stress Distribution and Fracture Lifespan on Enamel, Dentin, and Restorative Materials via Three-Dimensional Finite Element Analysis. *Polymers* **2023**, *15*, 1637. [CrossRef]
40. Costăchel, B.C.; Bechir, A.; Târcolea, M.; Mihai, L.L.; Burcea, A.; Bechir, E.S. The Stresses and Deformations in the Abfraction Lesions of the Lower Premolars Studied by the Finite Element Analyses: Case Report and Review of Literature. *Diagnostics* **2024**, *14*, 788. [CrossRef]

Disclaimer/Publisher's Note: The statements, opinions and data contained in all publications are solely those of the individual author(s) and contributor(s) and not of MDPI and/or the editor(s). MDPI and/or the editor(s) disclaim responsibility for any injury to people or property resulting from any ideas, methods, instructions or products referred to in the content.